creative commons
COMMONS DEED

저작자표시-비영리-변경금지 2.0 대한민국

이용자는 아래의 조건을 따르는 경우에 한하여 자유롭게

- 이 저작물을 복제, 배포, 전송, 전시, 공연 및 방송할 수 있습니다.

다음과 같은 조건을 따라야 합니다:

저작자표시. 귀하는 원저작자를 표시하여야 합니다.

비영리. 귀하는 이 저작물을 영리 목적으로 이용할 수 없습니다.

변경금지. 귀하는 이 저작물을 개작, 변형 또는 가공할 수 없습니다.

- 귀하는, 이 저작물의 재이용이나 배포의 경우, 이 저작물에 적용된 이용허락조건을 명확하게 나타내어야 합니다.
- 저작권자로부터 별도의 허가를 받으면 이러한 조건들은 적용되지 않습니다.

저작권법에 따른 이용자의 권리는 위의 내용에 의하여 영향을 받지 않습니다.

이것은 이용허락규약(Legal Code)을 이해하기 쉽게 요약한 것입니다.

Disclaimer

dCollection

A DISSERTATION
FOR THE DEGREE OF MASTER

Assessment of the pigeon (Columba livia) retina with spectral domain optical coherence tomography

Optical coherence tomography를 이용한 비둘기 망막 평가

August 2021

Graduate School of Veterinary Medcine
Seoul National University
Veterinary Clinical medicine Major

Sunhyo Kim

Assessment of the pigeon (*Columba livia*) retina with spectral domain optical coherence tomography

Optical coherence tomography를 이용한 비둘기 망막 평가

지도교수 서 강 문

이 논문을 수의학 석사 학위논문으로 제출함

2021년 4월

서울대학교 대학원

수의학과 임상수의학 전공

김 선 효

김선효의 석사 학위논문을 인준함

2021년 7월

위 원 장 _____

부 위 원 장 _____

위 원 _____

Assessment of the pigeon (Columba livia) retina with spectral domain optical coherence tomography

Supervised by

Professor Kangmoon Seo

Sunhyo Kim

Major in Veterinary Clinical Science,

Department of Veterinary Medicine Graduate School,

Seoul National University

Abstract

This study was performed to assess the normal retina of the pigeon eye using spectral-domain optical coherence tomography (SD-OCT) and to establish the normative reference.

Twelve eyes of ophthalmologically normal six pigeons (*Columba livia*) were included. SD-OCT images were taken with the dilated pupil under sedation. Four meridians, including the fovea, optic disc, red field, and yellow field, were obtained in each eye. The layers including full thickness (FT), ganglion cell complex (GCC), thickness from the retinal pigmented epithelium to the outer nuclear layer (RPE-ONL), and from the retinal pigmented epithelium to the inner nuclear layer (RPE-INL) were manually measured.

The average FT values were significantly different in all four meridians ($p < 0.05$) and the optic disc meridian was thickest (294.0 ± 13.9 μm). The average GCC was

thickest in the optic disc (105.3 ± 27.1 μm) and thinnest in the fovea meridian (42.8 ± 15.3 μm). The average RPE-INL of the fovea meridian (165.5 ± 18.3 μm) was significantly thicker than that of the other meridians ($p < 0.05$). The average RPE-ONL of the fovea, optic disc, yellow field, and red field were 91.2 ± 5.2 μm, 87.7 ± 5.3 μm, 87.6 ± 6.5 μm, and 91.4 ± 3.9 μm, respectively. RPE-INL and RPE-ONL thickness of the red field meridian did not change significantly depending on the measured location.

This study could provide the values of normative SD-OCT references for the diagnosis of pigeon retinopathies and further research on avian fundus structure.

Keywords: Fovea, optical coherence tomography, optic disc, pigeon, retina

***Student Number*: 2017-22364**

Contents

Introduction

Almost every bird is a highly visual animal with a few exceptions (Jones *et al*., 2007). As visual performance is crucial for their lives, the fundus examination and vision research are important in avian medicine. Indirect and direct ophthalmoscopes are commonly used for fundus examination, similar to that for other animals. However, these instruments can provide limited diagnostic information, and might not be enough to make a specific diagnosis on the status of the avian retina (Azmanis *et al.,* 2015). Optical coherence tomography (OCT), a noninvasive imaging technology, has been widely used in veterinary ophthalmology recently (Rauscher *et al*., 2013). As this imaging device provides in vivo cross-sections of the retina with high resolution, it is effectively used for clinical diagnosis and research of various animal eyes including birds (Rauscher *et al*., 2013; McLellan and Rasmussen, 2012; Gelatt *et al*., 2013; Rosolen *et al*., 2012).

Basically, structures of all vertebrate retinas are similar, but birds have some specific features such as the pecten oculi, a specialized, nutritive structure with an avascular retina, and one or two foveae in their fundus (Jones *et al,.*2007). Although the histologic investigations of these avian retinal structures have been shown by several studies (Querubin *et al,.*2009), the retinal thickness could be distorted and unable to reflect the structure of the retina while the animal is alive. The enucleation of the eyes for histopathologic examination is also a clinical limitation. However, OCT scanning is more advantageous as it is non-invasive, suitable for serial monitoring, and reflects the distortion less tissue structure. A few examinations with OCT have been conducted in living birds (Rauscher *et al.,* 2013; Huang *et al.,* 1998; Moayed *et al.,* 2011; Ruggeri *et al.,* 2010) ; however no attempt to establish and

describe normal OCT data for specific avian species has been made. The purpose of this study was to assess the normal retinal structure of the pigeons using OCT images, measured manually to establish normative references.

Materials and Methods

1. Experimental animals

Twelve eyes of six pigeons (Columba livia) were enrolled in this study. Although their gender was not verified, all birds were adults, over a year old. The mean body weight of the pigeons was 278.0 ± 18.3 g (260~310 g). All procedures were performed with the approval of the Institutional Animal Care and Use Committee at Seoul National University (SNU-191002-5).

2. Ophthalmic examination and OCT scan

All pigeons were instilled with 1% rocuronium (Rocunium Inj.; Hana Pharm. Co., Ltd., Korea) topically (Baine *et al*., 2016; Petriz et al., 2016; Barsotti *et al*., 2010) for pupil dilation and sedated with intramuscular medetomidine injection (0.2 mg/kg; Dormitor®; Zoetis, Florham Park, NJ, USA). Ocular examinations, including slit-lamp bio microscopy (SL-D7®; Topcon Corp., Tokyo, Japan), rebound tonometry (TonoVet®; Icare, Tiolat, Helsinki, Finland), and funduscopy (Kowa Hand-held Fundus Camera®; Kowa Co., Tokyo, Japan) were conducted.

Following the ophthalmic examinations, spectral domain OCT (SD-OCT; Optovue®; iVue Inc., Freemont, CA, USA) images were taken using the 'retinal map scan mode' for both the eyes with the sedated pigeons manually restrained. During the OCT scan, the head of the pigeons was slightly bent ventrally, as the pecten oculi falls plumb down from the optic disc in the en face image. It helped each OCT image to be taken parallel to the line of two points, the fovea and optic disc (Figure 1). The eyes were kept moist with artificial tears during the OCT scanning.

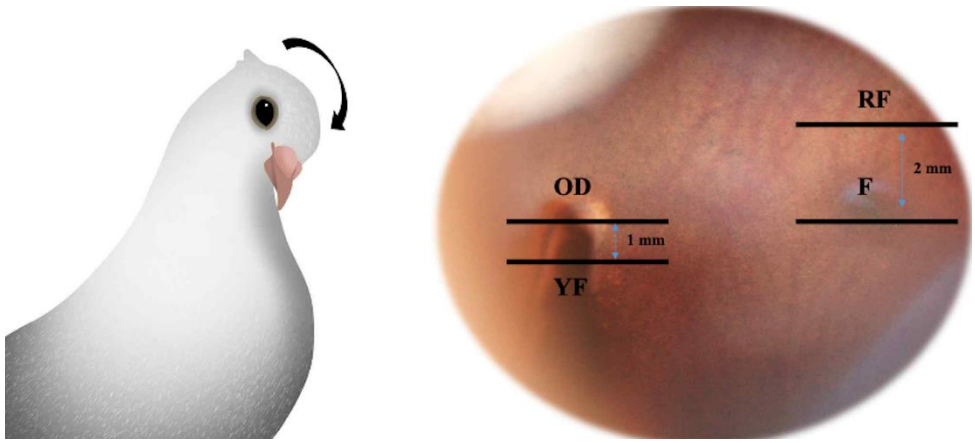

Fig. 1. Illustration image of the pigeon and the funduscopic image. Pigeon was restrained with the head slightly bent ventrally. Four meridians are represented on the funduscopic image. OD, optic disc; F, fovea; YF, yellow field; RF, red field.

3. Measurement

In this study, the pigeon retina was demonstrated in the four meridians including the fovea, optic disc, red field, and yellow field. Although the pigeon has variable and less well-differentiated fovea (Querubin *et al*., 2009), it can be easily detected on the nasal region from the optic disc. The red field of the retina, known as the area dorsalis of the pigeon, is one of the two major regions for vision with the fovea. High density of red oil droplets is in the cone cell in this area and the superior dorsal quadrant (Querubin *et al*., 2009). In this study, a meridian located 2 mm dorsally from the fovea represented the red field. The remainder of the pigeon retina, called the yellow field, was represented by a meridian located 1 mm ventrally from the optic disc. The fovea and optic disc images were taken at the center of the meridian (Figure 1).

Each eye was evaluated in the four areas including the fovea, optic disc, yellow field, and red field by the retina map scan mode, which was generally used to analyze the fovea and macular volume. It provided 20 horizontal cross-sections of the 6 x 6 mm retinal field and the average thickness with an early treatment diabetic retinopathy study (ETDRS) grid. As the center of the ETDRS grid could be moved to the desired position, it helped in choosing the meridian, which was some distance away from the objective points such as the fovea and optic disc for the measurement. The thickness of the layers was manually measured at five locations (0 mm, ± 1 mm, ± 2 mm) based on the center of each meridian (nasal and temporal were marked + and −, respectively). Four layers including full retinal thickness (FT; from

the retinal pigmented epithelium [RPE] to the inner limiting membrane), thickness of the ganglion cell complex (GCC; from the inner limiting membrane to the ganglion cell layer [GCL]), thickness of photoreceptor minus its axon (RPE-ONL; from RPE to outer nuclear layer), and thickness from the RPE to the inner nuclear layer (RPE-INL) were measured in all meridians. Only high-quality images were chosen, and the data were measured using the software included in the OCT device.

4. Histological examination

To identify the histological structure of the pigeon retina, a globe was fixed with formalin and stained with hematoxylin and eosin.

5. Statistical analyses

All statistical analyses were performed using commercial statistical software (R version 3.4.1). For describing statistical data, means, standard deviations (SD), and confidence intervals of 95% were used. Comparison of the layer thicknesses from each location and average thickness across the meridians were carried out using one-way ANOVA. Pairwise comparisons across the locations were adjusted for multiple comparisons using the post hoc Tukey test in all four meridians.

Results

1. Ophthalmic examination

There was no abnormality in all eyes on intraocular pressure (IOP) measurement, slit-lamp biomicroscopic, or funduscopic examination. The mean IOP was 11.7 ± 1.7 mm Hg within normal range in all the eyes.

2. Histological evaluation

Histological segmentation of the pigeon retina was shown in Figure 2, and all the retinal layers could be observed. The NFL was thicker near the pecten, and the thickness varied greatly depending on the location. The GCL consisted of about 1~3 nuclear layers and appeared thicker near the fovea. The INL and ONL consisted of approximately 9~20 and 2~4 nuclear layers, respectively. The IPL and INL occupied more than 50% of the whole retinal thickness, and the outer plexiform layer (OPL) was not very developed. At most locations, the RPE and photoreceptor layer were separated during the slide production process.

3. The SD-OCT images

All retinal layers could be identified and are presented in Figure 2. The four meridians including the fovea, optic disc, yellow field and red field were taken and are presented in Figures 3~6. The details of each layer are as follows. Because the OCT was not able to visualize the structure under the pecten, the images had shadows in the middle of the optic disc and yellow field meridians.

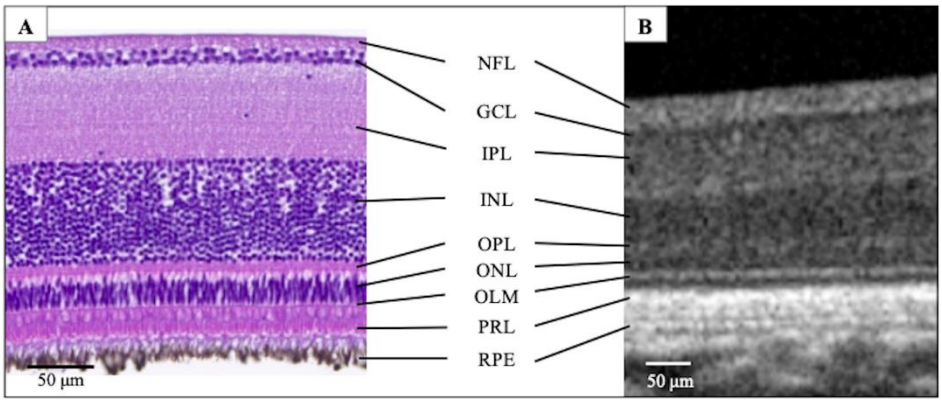

Fig. 2. Histologic segmentation of the pigeon retina (A) and the corresponding image scanned with optical coherence tomography device (B). NFL, nerve fiber layer; GCL, ganglion cell layer; IPL, inner plexiform layer; OPL, outer plexiform layer; ONL, outer nuclear layer; ELM, external limiting membrane; PRL, photoreceptor layer; RPE, retinal pigment epithelium.

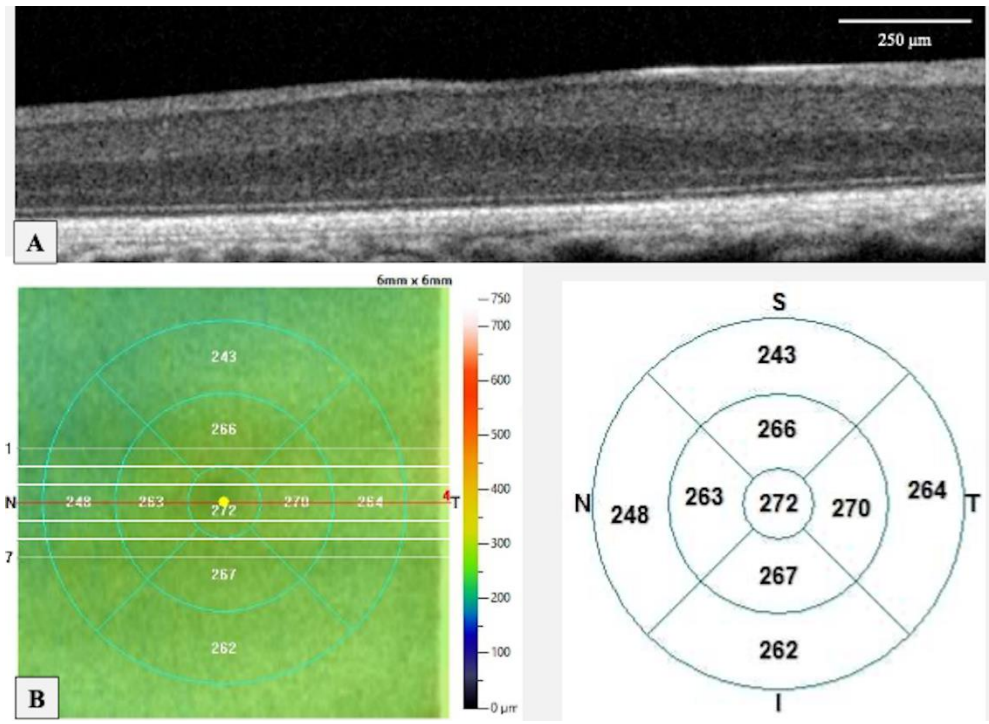

Fig. 3. Retina map optical coherence tomography (OCT) scan of the pigeon OS. (A) Tomographic image of the fovea meridian. Fovea is seen as a small pit at the center of the image. A scale bar to the right is present. (B) Normal database (NDB) reference map with the early treatment diabetic retinopathy study (ETDRS) grid and associated values on the right circle. ETDRS grid was repositioned on the center of the fovea. Color scale of NDB reference represents normative data in human. Red line corresponds to the fovea meridian which is shown in (A). S, superior; T, temporal; I, inferior; N, nasal.

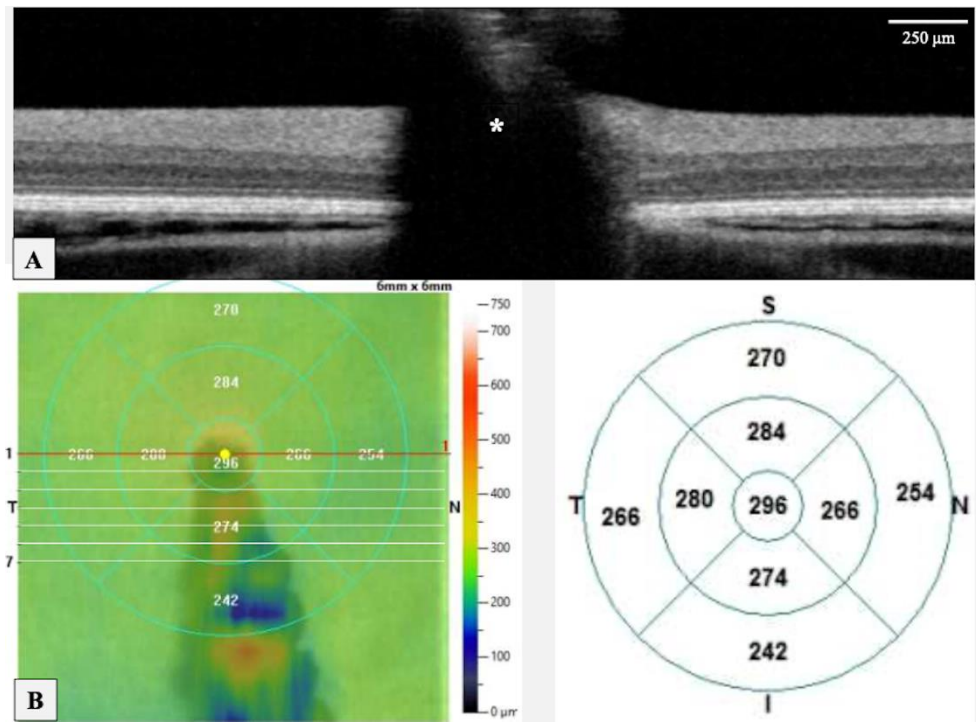

Fig. 4. Retina map optical coherence tomography (OCT) scan of the pigeon OD. (A) Tomographic image of the optic disc meridian. Structure under the pecten (*) was not visualized on the OCT image. A scale bar to the right is present. (B) Normal database (NDB) reference map with the early treatment diabetic retinopathy study (ETDRS) grid and associated values on the right circle. ETDRS grid was repositioned at the center of the optic disc where the pecten originated. Color scale of NDB reference represents normative data in human. Red line corresponds to the optic disc meridian which is shown in (A). S, superior; T, temporal; I, inferior; N, nasal.

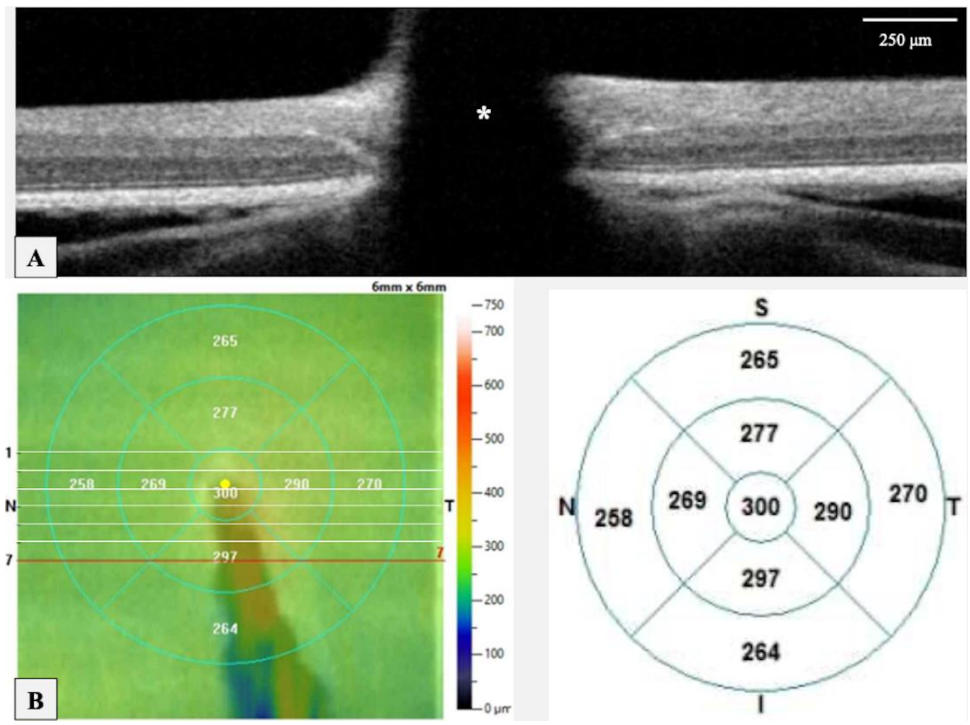

Fig. 5. Retina map optical coherence tomography (OCT) scan of the pigeon OS. (A) Tomographic image of the yellow field meridian. Structure under the pecten (*) was not visualized on the OCT image. A scale bar to the right is present. (B) Normal database (NDB) reference map with the early treatment diabetic retinopathy study (ETDRS) grid and associated values on the right circle. ETDRS grid was repositioned at the center of the optic disc where the pecten originated. Color scale of NDB reference represents normative data in human. Red line corresponds to the optic disc meridian which is shown in (A). S, superior; T, temporal; I, inferior; N, nasal.

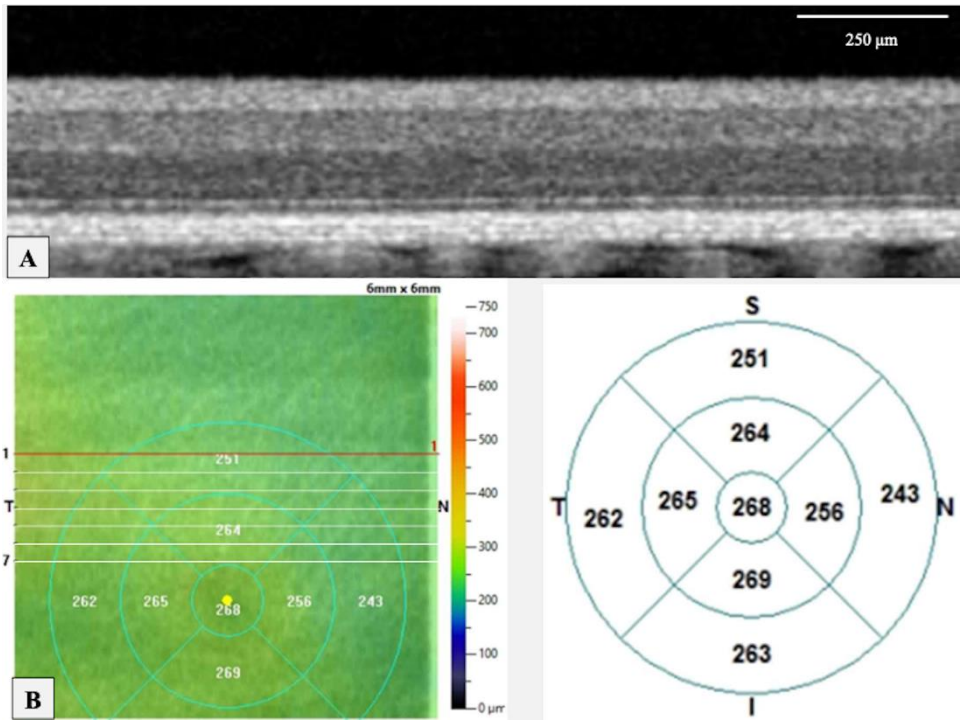

Fig. 6. Retina map optical coherence tomography (OCT) scan of the pigeon OD. (A) Tomographic image of the red field meridian. A scale bar to the right is present. (B) Normal database (NDB) reference map with the early treatment diabetic retinopathy study (ETDRS) grid and associated values on the right circle. ETDRS grid was repositioned at the center of the fovea. Color scale of NDB reference represents normative data in human. Red line corresponds to the red field meridian which is shown in (A) and this is located 2 mm dorsally from the fovea. S, superior; T, temporal; I, inferior; N, nasal.

4. Full thickness (FT)

The FT of the pigeon retina in all meridians was presented in Table 1. The average FT of the fovea meridian was 275.3 ± 11.2 μm. The fovea was noticeable as a small pit about 1 mm diameter in nasal from the optic disc. Although there was little variation depending on the location, the 2 mm region was significantly thinner than the other regions in this meridian. The average FT of the optic disc and yellow field meridians were 294.0 ± 13.9 μm and 284.3 ± 10.2 μm, respectively. The FT of the ± 1 mm region was significantly thicker than the ± 2 mm region ($P < 0.05$), and these meridians were symmetrical about pecten. The average FT of the red field meridian was 261.1 ± 6.6 μm and it was the thinnest among the meridians.

Table 1. Measured pigeon retinal full thickness in 4 meridians (μm)

	Temporal				Nasal				Average
Location	-2 mm	-1 mm	0 mm		1 mm	2 mm			
Fovea	278.3 ± 5.2^{b*}	283.8 ± 7.3^{b}	279.0 ± 5.8^{b}		278.0 ± 7.5^{b}	257.3 ± 5.9^{a}			275.3 ± 11.2^{b}
Optic disc	287.9 ± 8.0^{a}	310.7 ± 6.8^{c}	–		296.9 ± 9.8^{b}	280.3 ± 8.0^{a}			294.0 ± 13.9^{d}
Yellow field	280.4 ± 6.4^{ab}	293.8 ± 8.4^{c}	–		287.4 ± 9.3^{bc}	275.3 ± 6.0^{a}			284.3 ± 10.2^{c}
Red field	266.3 ± 8.4^{c}	263.0 ± 5.5^{bc}	258.9 ± 5.4^{ab}		255.9 ± 3.7^{a}	261.3 ± 4.3^{ac}			261.1 ± 6.6^{a}

*: mean ± SD

a, b, c: Different superscript letters mean significant differences in the same meridian and average column, respectively ($p < 0.05$).

Note: At the center of optic disc and yellow field meridians, measuring was not possible because of the pecten.

5. Ganglion cell complex (GCC) thickness

GCC thickness of the pigeon retina in all meridians is presented in Table 2. The average GCC thickness of the fovea meridian was 42.8 ± 15.3 μm. GCC of the fovea (0 mm) was significantly thinner than that of the other regions within this meridian ($p < 0.05$). The retinal ganglion cell layer of the fovea was thicker than that in the peri-foveal region, but the nerve fiber layer was thinner than in the other regions. The average GCC thickness of the optic disc and yellow field meridian were 105.3 ± 27.1 μm and 95.8 ± 22.4 μm, respectively. GCC of ± 1 mm region of these meridians was significantly thicker than the ± 2 mm region ($p < 0.05$), indicating that the closer to the pecten, the thicker the GCC. The average GCC thickness of the red field meridian was 57.3 ± 7.8 μm.

Table 2. Measured pigeon retinal ganglion cell complex thickness in 4 meridians (μm)

	Temporal				Nasal				Average
Location	-2 mm	-1 mm	0 mm		1 mm		2 mm		
Fovea	60.0 ± 10.4^{c}	37.6 ± 10.7^{b}	25.3 ± 6.8^{a}		42.7 ± 14.0^{b}		48.3 ± 8.5^{bc}		42.8 ± 15.3^{a}
Optic disc	98.8 ± 9.8^{ab}	135.9 ± 9.6^{c}	−		107.3 ± 10.8^{b}		79.3 ± 32.0^{a}		105.3 ± 27.1^{c}
Yellow field	93.0 ± 7.2^{b}	121.7 ± 16.6^{c}	−		99.3 ± 13.7^{b}		69.1 ± 9.5^{a}		95.8 ± 22.4^{c}
Red field	64.6 ± 8.0^{c}	59.3 ± 6.0^{bc}	52.9 ± 6.3^{ab}		50.9 ± 4.4^{a}		58.7 ± 6.0^{bc}		57.3 ± 7.8^{b}

*: mean ± SD

a, b, c: Different superscript letters mean significant differences in the same meridian and average column, respectively ($p < 0.05$).

Note: At the center of optic disc and yellow field meridians, measuring was not possible because of the pecten.

6. Retinal pigmented epithelium to inner nuclear layer (RPE-INL) thickness

The RPE-INL thickness of the pigeon retina in all meridians was presented in Table 3. The average RPE-INL thickness was the thickest in the fovea meridian, and it was 165.5 ± 18.3 μm ($p < 0.05$). At the fovea, the central region of this meridian (0 mm), RPE-INL thickness was significantly thicker than the other regions ($p < 0.05$). The average RPE-INL thickness of the optic disc and yellow field meridians was 138.7 ± 10.2 μm and 136.8 ± 10.9 μm, respectively, and they were not significantly different. In the ± 1 mm region, RPE-INL was significantly thinner than the ± 2 mm region in these meridians. The average RPE-INL thickness of the red field meridian was 146.1 ± 3.1 μm. The RPE-INL of this meridian had no significant difference depending on the measured location.

Table 3. Measured RPE-INL thickness of the pigeon retina in 4 meridians (μm)

	Temporal			Nasal		Average
Location	-2 mm	-1 mm	0 mm	1 mm	2 mm	
Fovea	151.7 ± 5.6[a]	169.8 ± 7.2[b]	195.3 ± 8.7[c]	162.7 ± 8.9[b]	148.0 ± 3.9[a]	165.5 ± 18.3[c]
Optic disc	137.8 ± 5.8[b]	128.4 ± 8.6[a]	−	138.5 ± 7.6[b]	150.0 ± 5.2[c]	138.7 ± 10.2[a]
Yellow field	135.8 ± 6.6[b]	125.1 ± 9.1[a]	−	139.6 ± 8.0[b]	146.6 ± 7.1[c]	136.8 ± 10.9[a]
Red field	144.9 ± 3.4[a]	146.3 ± 2.9[a]	147.7 ± 3.3[a]	146.3 ± 2.9[a]	145.0 ± 2.7[a]	146.1 ± 3.1[b]

*: mean ± SD

a, b, c: Different superscript letters mean significant differences in the same meridian and average column, respectively ($p < 0.05$).

Note: At the center of optic disc and yellow field meridians, measuring was not possible because of the pecten.

7. Retinal pigmented epithelium to outer nuclear layer (RPE-ONL) thickness

The RPE-ONL thickness of the pigeon retina in all meridians was presented in Table 4. The average RPE-ONL thickness of the fovea and red field meridians were 91.2 ± 5.2 μm and 91.4 ± 3.9 μm, respectively, which were not significantly different. There was no significant difference in RPE-ONL thickness depending on the location in the fovea and red field meridians. The average RPE-ONL thickness of the optic disc and yellow field meridians were 87.7 ± 5.3 μm and 87.6 ± 6.5 μm, respectively, which were not significantly different.

Table 4. Measured RPE-ONL thickness of the pigeon retina in 4 meridians (μm)

	Temporal			Nasal		Average
Location	-2 mm	-1 mm	0 mm	1 mm	2 mm	
Fovea	90.6 ± 4.6[a]	92.3 ± 5.4[a]	93.7 ± 5.5[a]	88.5 ± 5.5[a]	91.0 ± 3.9[a]	91.2 ± 5.2[b]
Optic disc	87.7 ± 4.0[ab]	84.8 ± 5.3[a]	−	87.6 ± 5.9[ab]	90.7 ± 4.7[b]	87.7 ± 5.3[a]
Yellow field	87.8 ± 5.0[ab]	82.3 ± 6.8[a]	−	88.4 ± 6.6[ab]	92.0 ± 3.6[b]	87.6 ± 6.5[a]
Red field	90.7 ± 4.1[a]	91.3 ± 3.1[a]	92.0 ± 3.6[a]	91.3 ± 5.1[a]	91.7 ± 3.6[a]	91.4 ± 3.9[b]

*: mean ± SD

a, b, c: Different superscript letters mean significant differences in the same meridian and average column, respectively ($p < 0.05$).

Note: At the center of optic disc and yellow field meridians, measuring was not possible because of the pecten.

Discussion

Conventional examination of the retinal structure in birds relied on ophthalmoscopy or histologic examination, which was inevitable for enucleation. Furthermore, histopathological examination could have some artifacts, especially in measuring the thickness of the NFL because of tissue swelling, autolysis, shrinkage, and inadvertent oblique sectioning during specimen prepared (Frankel *et al*., 2005). In this study, not only NFL, the other layers could also be evaluated reliably in the OCT images. Compared with the histologic evaluation, the tomographic image of the OCT showed the retinal layer structure well; rather, it was possible to visualize the distorted parts in the histology.

Previous OCT studies in various animals have provided valuable information to estimate the normal structures (Azmanis *et al*., 2015; McLellan and Rasmussen, 2012; Mariani, 1987). We could find all the retinal layers in the OCT images of pigeons like other vertebrae in this study. However, the OPL was thin and its boundaries were unclear in all meridians, which meant that the outer border of the INL and the inner border of the ONL might be inaccurate. For this reason, the distance from the outer border of the RPE to the inner border of the INL was measured to estimate the INL. Previous study reported that the OPL of the pigeon retina was a tri-stratified structure because the photoreceptors end at three different levels (Mariani, 1987). This stratification arranges the dendrites of the bipolar and horizontal cells in a lamellar structure. Unclear boundaries of the OPL might reflect this anatomical characteristic. The limitation was that the inner boundary of the ONL was unclear, but to measure the thickness of the photoreceptor cells, the distance from the outer border of the RPE to the inner border of the ONL was measured in

this study. OPL was not included for photoreceptor thickness as it was dependent on the neurons of the bipolar and horizontal cells as in the previous study (Ofri and Ekesten, 2020).

The fovea, one of the distinguishing structures of birds with the domestic animals, is an area for high visual acuity, which differs among species (Mariani, 1987). The fovea of the pigeon retina in the current study was a shallow saucer-shaped depression, and is termed the anthropoid type. This type of fovea can be seen in primates and the temporal fovea of some bifoveate birds. The other type of fovea, known as the convexiclivate, is deep and funnel or whirlpool-shaped and commonly found in fish, reptiles, and birds (Pumphrey, 1948). The anthropoid-type of pigeon retina in this study showed statistically insignificant FT compared with the peri-foveal region, contrary to the convexiclivate fovea, observed in the previous study having notably decreased FT at the fovea due to the absence of all retinal layers proximal to the ONL (Espinheira *et al*., 2020). The correlation between the shape of the fovea and its function has been still incompletely understood (Bringmann, 2019).

The fovea and red field are high visual acuity regions in the pigeon retina, having similar mean visual acuity measured behaviorally (Querubin *et al*., 2009; Hodos *et al*., 1985; Hodos *et al*., 1991). It has been reported that pigeons have 350-400 μm diameter rod-free regions at the center of the fovea, colocalizing with the highest cone cell density in the photoreceptor layer. Likewise, the red field also has 1.3-3 times higher cone cell density compared with the yellow field (Querubin *et al*., 2009) It is known as the single cone cell synapses with a single bipolar cell for higher visual resolution, whereas several rods converge upon a single bipolar cell (Maggs *et al*., 2018). For these reasons, INL, which represents the bipolar cell bodies, could be

thick at the fovea and red field meridian. In this study, RPE-INL of the fovea and red field were significantly thicker than that of the optic disc and yellow field meridian. In the cone-rich retina of most domestic animals, the number of bipolar cells increase remarkably, similar to the amacrine cells (Gelatt *et al*., 2013). As the rod cell density of the pigeon retina is known to be invariable in all retinal fields except the rod-free region at the center of the fovea (Querubin *et al*., 2009), the difference in cone cell density seems to be reflected in the pigeon INL thickness.

When comparing the thicknesses of the pigeon retinal layers, including FT, GCC, and RPE-INL, the location of measurement was critical, as a significant difference existed depending on the meridian (Tables 1~3). In particular, GCC thickness was highly variable and affected FT in this study. For this reason, comparing only FT might be effective in some diseases primarily affecting GCC, such as glaucoma, but might be less sensitive to retinopathies affecting photoreceptors first. Unlike FT, the absolute difference in the average RPE-ONL thickness was not significant among the meridians, although the fovea and red field meridians were statistically thicker than those of the optic disc and yellow field meridians (Table 4). This suggested that the pigeon retina had a comparatively uniform layer thickness of the photoreceptor cell bodies regardless of the rod and cone density.

As it was difficult to measure the GCL alone accurately in the pigeon retina, its measurement was done representatively in this study. However, unlike other regions, the GCL of the fovea was thick enough to be realized in the foveal meridian. This tendency was similar to a previous histopathological report that showed the ganglion cell density of the fovea higher than that in the other regions (Querubin *et al*., 2009). It was also related to high pigeon cone cell density in the fovea. The convergence of

the cone cell onto the ganglion cell ratio was known as 2.1 in the fovea and the other field was > 4.6 (Querubin *et al*., 2009). This could be the reason the GCL of the red field meridian was not as remarkable as that of the fovea.

One of the main purposes of this study was to set the normative reference of normal pigeon retinal thickness using OCT imaging, which could be used in the diagnosis of pigeon retinopathies and further studies on avian fundus structure. Many retinal disorders are known to primarily affect specific retinal layer components. Although the cellular composition of each meridian was different, the red field meridian was considered as the ideal region to set the normative reference index for screening. This meridian was one of the regions with high visual cell density and showed the least variation in RPE-ONL and RPE-INL thickness depending on the location (Tables 3, 4). If the thickness of retinal layers changed drastically depending on the measured location in some meridians, they might be inadequate for representing average as they could be easily altered with each measurement. Evaluating GCC thickness and its structure could be advantageous in the fovea meridian and an additional study comparing affected pigeons with the normal might be conducted.

The small number and the confined specific age of the pigeons were the most significant limitations of this study. It was reported that the number and the acuity of photoreceptors of pigeon decreased with age (Fitzgerald *et al*., 2001). All pigeons in this study were over one years. As a previous report to generate baseline OCT measurements of other species retinas, groups categorized by age could be needed in further research (Ofri and Ekesten, 2020). Despite these limitations, this study might provide a valuable index of pigeon retinal examination and research. It could

be used for further studies, such as various retinal diseases of pigeon or setting the normative index of other species.

Conclusion

Tomographic images of the living pigeon retina could be obtained using SD-OCT in this study. The measured values could provide the normative SD-OCT references for the diagnosis of pigeon retinopathies and further research on avian fundus structure. Furthermore, it is considered that the methodology used in this study could be applied to other studies to establish normative SD-OCT reference in various animal retina.

References

Azmanis P, Rauscher FG, Werner B, et al. The additional diagnostic value of optical coherence tomography (OCT) and its application procedure in a wide variety of avian Species. J Clin Exp Ophthalmol 2015;6:431.

Baine K, Hendrix DVH, Kuhn SE, et al. The efficacy and safety of topical rocuronium bromide to induce bilateral mydriasis in hispaniolan amazon parrots (Amazona ventralis). J Med Surg Med 2016;30:8-13.

Barsotti G, Briganti A, Spratte JR, et al. Mydriatic effect of topically applied rocuronium bromide in tawny owls (Strix aluco): comparison between two protocols. Vet Ophthalmol 2010;13:9-13.

Bringmann A. Structure and function of the bird fovea. Anat Histol Embryol 2019;48:177-200.

Espinheira GF, Abou-Madi N, Ledbetter EC, et al. Spectral-domain optical coherence tomography imaging of normal foveae: A pilot study in 17 diurnal birds of prey. Vet Ophthalmol 2020;23:347-357.

Fitzgerald ME, Tolley E, Frase S, et al. Functional and morphological assessment of age-related changes in the choroid and outer retina in pigeons. Vis Neurosci 2001;18:299-317.

Frenkel S, Morgan JE, Blumenthal EZ. Histological measurement of retinal nerve fibre layer thickness. Eye 2005;19:491-498.

Gelatt KN, Gilger BC, Kern TJ. Veterinary Ophthalmology, 5th edn. Ames, IA:

Wiley-Blackwell; 2013;39-668.

Hodos W, Bessette BB, Macko KA, et al. Normative data for pigeon vision. Vision Res 1985;25:1525-1527.

Hodos W, Miller RF, Fite KV. Age-dependent changes in visual acuity and retinal morphology in pigeons. Vision Res 1991;31:669-677.

Huang Y, Cideciyan AV, Papastergiou GI, et al. Relation of optical coherence tomography to microanatomy in normal and rd chickens. Invest Ophthalmol Vis Sci 1998;39:2405-2416.

Jones MP, Pierce KE Jr, Ward D. Avian vision: a review of form and function with special consideration to birds of prey. J Exot Pet Med 2007;16:69-87.

Maggs DJ, Miller PE, Ofri R. Slatter's Fundamentals of Veterinary Ophthalmology. 6th edn. St. Louis, MO: Elsevier Inc; 2018:347-398.

Mariani AP. Neuronal and synaptic organization of the outer plexiform layer of the pigeon retina. Am J Anat 1987;179:25-39.

McLellan GJ, Rasmussen CA. Optical coherence tomography for the evaluation of retinal and optic nerve morphology in animal subjects: practical considerations. Vet Ophthalmol 2012;15:13-28.

Moayed AA, Song ES, Bizheva K, et al. In vivo volumetric imaging of chicken retina with ultrahigh-resolution spectral domain optical coherence tomography. Biomed Opt Express 2011;2:1268-1274.

Ofri R, Ekesten B. Baseline retinal OCT measurements in normal female beagles:

The effects of eccentricity, meridian, and age on retinal layer thickness. Vet Ophthalmol 2020;23:52-60.

Petritz OA, Guzman DS-M, Gustavsen K, et al. Evaluation of the mydriatic effects of topical administration of rocuronium bromide in Hispaniolan Amazon parrots (Amazona ventralis). J Am Vet Med Assoc 2016;248:67-71.

Pumphrey RJ. The theory of the fovea. J Exp Biol 1948;25:299-312.

Querubin A, Lee HR, Provis JM, et al. Photoreceptor and ganglion cell topographies correlate with information convergence and high acuity regions in the adult pigeon (Columba livia) retina. J Comp Neurol 2009;517:711-722.

Rauscher FG, Azmanis P, Körber N, et al. Optical coherence tomography as a diagnostic tool for retinal pathologies in avian ophthalmology. Invest Ophthalmol Vis Sci 2013;54:8259-8269.

Rosolen SG, Rivière MLK, Lavillegrand S, et al. Use of a combined slit-lamp SD-OCT to obtain anterior and posterior segment images in selected animal species. Vet Ophthalmol 2012;15:105-115.

Ruggeri M, Major JC, McKeown C, et al. Retinal structure of birds of prey revealed by ultra-high resolution spectral-domain optical coherence tomography. Invest Ophthalmol Vis Sci 2010;51:5789-5795.

국문 초록

Optical coherence Tomography를 이용한 비둘기 망막 평가

지도교수 서 강 문

김 선 효

서울대학교 대학원

수의학과 임상수의학 전공

본 연구는 광간섭단층촬영(SD-OCT)장비를 이용하여 비둘기 눈의 정상 망막을 평가하고 정상참고범위를 설정하기 위해 진행되었다.

안검사 상 정상인 비둘기 6마리의 12개 안구를 이용하였다. 진정하에 동공을 산동시킨 후 광간섭단층촬영을 진행하였다. 망막중심오목, 시신경유두, 적색영역(red field), 황색영역(yellow field)의 4가지 단면을 각각의 안구에서 촬영하였다. 전체 두께(full thickness), 신경절세포층집합(ganglion cell complex), 망막색소상피부터 바깥핵층(retinal pigmented epithelium to the outer nuclear layer), 망막색소

상피부터 속핵층(retinal pigmented epithelium to the inner nuclear layer)를 직접 측정하였다.

전체 두께의 평균값은 4가지 단면에서 유의적으로 차이가 있었으며($p < 0.05$), 시신경유두단면에서 가장 두꺼웠다(294.0 ± 13.9 μm). 평균 신경절세포층집합은 시신경유두단면에서 가장 두꺼웠으며(105.3 ± 27.1 μm) 망막중심오목단면에서 가장 얇았다(42.8 ± 15.3 μm). 망막중심오목단면의 평균 망막색소상피부터 속핵층의 두께(165.5 ± 18.3 μm)는 다른 단면에서보다 유의적으로 두꺼웠다($p < 0.05$). 망막중심오목단면, 시신경유두단면, 황색영역단면과 적색영역단면의 평균 망막색소상피부터 바깥핵층의 두께는 각각 91.2 ± 5.2 μm, 87.7 ± 5.3 μm, 87.6 ± 6.5 μm, and 91.4 ± 3.9 μm 였다. 적색영역단면에서 망막색소상피부터 속핵층과 망막색소상피부터 바깥핵층의 두께는 측정 위치에 따라 유의적인 차이를 보이지 않았다.

본 실험에서 측정된 결과값은 비둘기의 망막병증을 진단하고 비둘기 안저 연구에 대한 후속 연구에 있어 정상참고범위로 활용될 수 있을 것으로 판단된다.

주요어 : 망막중심오목, 광간섭단층촬영, 시신경유두, 비둘기, 망막

학 번 : 2017-22364